Controllable Formation from Graphene Quantum Dots to Carbon nanotubes by Ionsputtering assisted Chemical Vapor Deposition

Jun Mok Ha*, In Mok Yang, Junhyeok Seo, Chan Young Lee, Yong Seok Hwang, Jae Kwon Suk, Jun Kue Park, Myung-Hwan Jung, and Sunmog Yeo

Particle Beam Research Division, Korea Multi-purpose Accelerator Complex (KOMAC), Korea Atomic Energy Research Institute (KAERI), 181 Mirae-ro, Geonchon-eup, Gyeongju, Gyeongbuk, 38180, Korea *Corresponding author: jmha@kaeri.re.kr

1. Introduction

Carbon allotropes are one of the most important issues in material science because they have versatile properties and are scientific topics of crucial importance. Among the allotropes, the zero-dimensional graphene quantum dots (GQDs) and the one-dimensional carbon nanotubes (CNTs) have attracted worldwide attention due to their diverse applications. For GQDs, their advantages such as stable fluorescence, outstanding biocompatibility, low toxicity, low cost, and high surface area have led to optical displays, sensors, bioimaging drug delivery, and photo-catalysts. On the other hand, CNTs have unique mechanical, electrical, and optical properties like high tensile strength, ultra-light weight, special electronic structures, and high chemical and thermal stability. These properties have made them useful for diverse applications such as nano-electronic devices, energy storage devices, composite materials, medicine, air and water filtering, and sensors. Since GQDs and CNTs are independently important research topics, the synthesis methods for GQDs and CNTs have been developed individually.

Although many synthesis methods have been developed and studied in depth individually, to the best of our knowledge, no research has been reported that both GQDs and CNTs were successfully synthesized in series by regulating the synthesis parameters. In this paper, we present a simple and convenient route from GQDs to CNTs by an ion-sputtering assisted chemical vapor deposition (CVD). Since this method can be easily applied to array and patterning processes, this study is extremely useful when a device requires both properties of GQD and CNT. Furthermore, the opposite electrical characteristics of GQDs and CNTs suggest that by fine-tuning the synthesis parameters, quantum criticality could be achieved at a certain point associated with the metal-insulator transition. This study also offers valuable insights into the topology of transforming zerodimensional GQDs into one-dimensional CNTs through manipulation of synthesis parameters.

2. Methods and Results

In this section, the detailed procedures of controllable formation from GQDs to CNTs by ion-sputtering assisted CVD are described.

2.1 Synthesis process for carbon allotropes through ion-sputtering assisted CVD

The carbon allotropes were fabricated by an ion-sputtering assisted CVD method that combined both the advantages of the ion-sputtering and CVD techniques, as schematically shown in Fig. 1. When the Pt-deposited Si substrate (PtDS) was annealed at a sufficiently high temperature, the deposited Pt thin film was dewetted and agglomerated to form many nanometer-sized particles. This led to the formation of Pt nanoparticles (PtNPs), which can act as catalysts to grow carbon allotropes. The shape of the allotropes can be effectively tailored from GQDs to CNTs by controlling the formation condition.

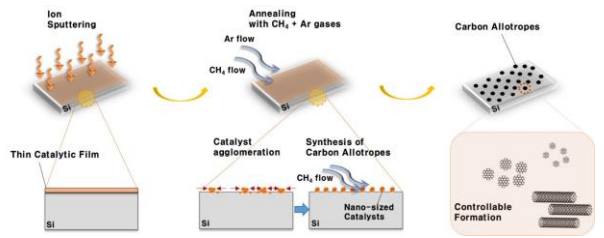


Fig. 1. A schematic layout of a synthetic process for the carbon allotropes through our ion-sputtering assisted CVD method. During the annealing process, the deposited Pt thin film was changed to PtNPs, which acted as catalysts to synthesize from GQDs to CNTs.

2.1 Controllable formation from GQDs to CNTs by ionsputtering assisted CVD

The FESEM, TEM, and AFM data display the GQDs prepared by our ion-sputtering assisted CVD method shown in Fig. 2. Pt ions were deposited on Si substrates through the ion-sputtering with an energy of 2 keV and a dose of 6.2×10^{13} #/cm². When the PtDS was annealed at 900 °C for 20 min with a gas mixture of Ar (100 sccm) and CH₄ (25 sccm), small-sized GQDs newly appeared on the surface of the Si substrate (Fig. 2a). The TEM and magnified images (Fig. 2b, c) obviously showed fabricated GQDs with a small spot shape. Furthermore, the HRTEM image and FFT pattern of the GQDs (Fig. 2c and inset) reveal that they had a crystalline structure and a uniform particle size with an average diameter of 7.88 ± 2.29 nm (Fig. 2d). Figure 2e shows the typical AFM image of the GQDs, and the

measured location is indicated by the yellow-dashed line representing randomly chosen GQDs. From the AFM data of the GQDs shown in Fig. 2e, f, it can be seen that the heights of the GQDs ranged from 0.5 to 4.4 nm (inset of Fig. 2e), and the average value was 1.97 ± 0.13 nm (Fig. 2f). A HRTEM image of the GQDs displayed lattice fringes with ~ 0.33 nm spacing (Fig. 3), which corresponded to (002) planes of graphite, suggesting that the GQDs have a disk-shaped morphology and consist of a few layers of graphene.

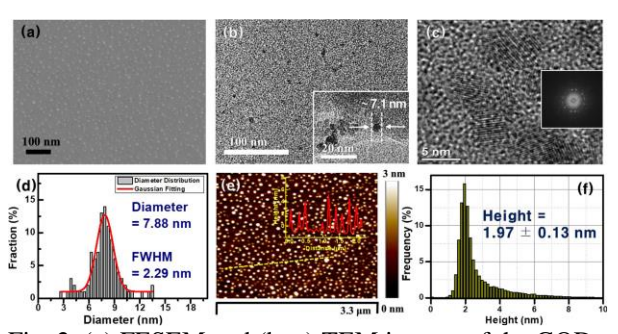


Fig. 2. (a) FESEM and (b, c) TEM images of the GQDs. The size of the fabricated GQDs is ~ 7.1 nm (inset of (b)). (c) The magnified TEM image of the GQDs and its corresponding FFT pattern (inset). (d) The diameter distribution of the GQDs. The red line is the Gaussian fit curve. The average size of the GQDs and the full width at half-maximum (FWHM) of the Gaussian curve are 7.88 and 2.29 nm, respectively. (e) A typical AFM image of the GQDs. The height distribution of the GQDs in e and the measured location is indicated by a yellow-dashed line (inset). (f) Height distribution of the fabricated GQDs on a whole surface of the Si substrate.

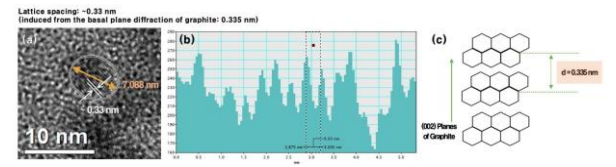


Fig. 3. HRTEM images and line profile analysis of the GQDs. (a) The HRTEM image of the GQD and (b) its corresponding line profile analysis (indicated by orange line). The size and lattice spacing of GQDs are 7.088 and ~0.33 nm, respectively. (c) The lattice fringe (d = 0.335 nm) is induced from the basal plane diffraction of graphite.

The shape of the carbon allotropes can be effectively controlled by changing the dose of Pt ions and the annealing conditions. To investigate the effects of a Ption dose on the growth of carbon allotropes, the allotropes were fabricated using different amounts of Pt ions. Figure 4 displays the FESEM images of the carbon allotropes synthesized at 900 °C for 20 min with a gas mixture of Ar (100 sccm) and CH₄ (25 sccm). The doses of the Pt ions deposited on the Si substrates were 7.4×10^{13} , 8.6×10^{13} , and 9.8×10^{13} #/cm², as shown in Fig. 4a–c, respectively. Compared to the small-sized GQDs

(ion dose = 6.2×10^{13} #/cm²) in Fig. 2, as the dose of the Pt ions increased, the size of the resultant GQDs was larger, and finally CNTs were generated through an intermediate step (Fig. 4). It is interesting to note that there were numerous bump-like white-spots on the apexes of the CNTs (Fig. 4c), and a few white-spots also existed at the intermediate step (Fig. 4b).

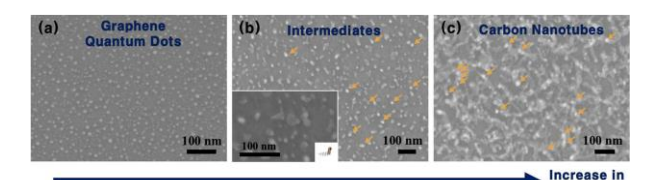


Fig. 4. FESEM images of the carbon allotropes synthesized by different amounts of Pt ions with doses of (a) 7.4×10^{13} , (b) 8.6×10^{13} , and 9.8×10^{13} #/cm², respectively. The Pt remnants (bright white-spots) are indicated by orange arrows in (b, c). Insets: schematics and magnified FESEM images.

In addition, Figure 5 shows the typical XPS survey spectra of the GQDs (Fig. 5a) and CNTs (Fig. 5b), and the XPS measurements were performed more than 20 times for the randomly chosen samples. The results of the XPS analysis clearly revealed that no Pt was left on the substrate, indicating the production of high-purity GQDs. On the other hand, the detectable Pt remained in the CNT samples.

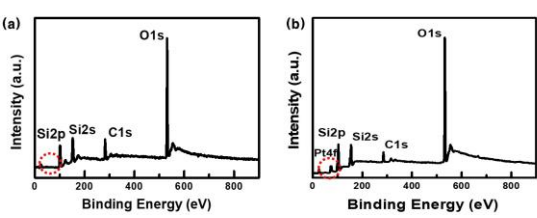


Fig. 5. Typical XPS spectra of the (a) GQDs and (b) CNTs on Si substrates, respectively. The positions of Pt4f peak are indicated by red circles in (a) and (b). The XPS measurements were performed more than 20 times for the randomly chosen samples.

3. Conclusions

We have presented a simple and convenient route to the synthesis mechanism from GQDs to CNTs by using an ion-sputtering assisted one-step annealing process. During the thermal annealing, the deposited Pt thin film changed to PtNPs, which act as catalysts and nucleation sites to synthesize carbon allotropes. Our synthesis method enables the controlled creation of carbon allotropes with the desired size, structure, and morphology by manipulating three key parameters (D, S, and T). The validity of these parameters was confirmed through experimental data conducted under various fabrication conditions. In addition, our bottom-up synthesis strategy makes it possible to generate pure

GQDs and CNTs with the cap of PtNPs, which is highly desirable in applications to industrial- and bio-fields. Another thing to note here is that the present work is the first report of the synthesis mechanism from GQDs to CNTs. Therefore, we believe that the present approach is very useful for diverse applications such as optoelectronics, nanophotonics, and sensing, as well as energy or environmental-related applications.

4. Acknowledgement

This work was supported through the National Research Foundation (NRF) of Korea (No. 2018R1D1A1B07050951), and KOMAC operation funds of KAERI by MSIT (Ministry of Science and ICT). This research was also supported by the National Research Council of Science & Technology (NST) grant by the Korea government (MSIT) (No. CAP23072-100).

REFERENCES

- [1] A. Hirsch, Nat. Mater. 9 (2010) 868-871.
- [2] Z. Wang, F. Dong, B. Shen, R. J. Zhang, Y. X. Zheng, L. Y. Chen, S. Y. Wang, C. Z. Wang, K. M. Ho, Y. Fan, B. Jin, W. Su, Carbon 101 (2016) 77-85.
- [3] X. Ye, M. Qi, M. Chen, L. Zhang, J. Zhang, Adv. Mater. Interfaces 10 (2023) 2201941.
- [4] R. Ye, C. Xiang, J. Lin, Z. Peng, K. Huang, Z. Yan, N. P. Cook, E. L. G. Samuel, C. Hwang, G. Ruan, G. Ceriotti, A. O. Raji, A. A. Martí, J. M. Tour, Nat. Commun. 4 (2013) 2943.
- [5] M. Semeniuk, Z. Yi, V. Poursorkhabi, J. Tjong, S. Jaffer, Z. Lu, M. Sain, ACS Nano 13 (2019) 6224-6255.
- [6] S. Chung, R. A. Revia, M. Zhang, Adv. Mater. 33 (2021) 1904362.
- [7] Y. Su, Y. Zhang, Carbon 83 (2015) 90-99.
- [8] S. Rathinavel, K. Priyadharshini, D. Panda, Mater. Sci. Eng. B 268 (2021) 115095.
- [9] D. Sun, C. Liu, W. Ren, H. Cheng, Small 9 (2013) 1188-1205.
- [10] C. M. Luk, L. B. Tang, W. F. Zhang, S. F. Yu, K. S. Teng, S. P. Lau, J. Mater. Chem. 22 (2012) 22378-22381.
- [11] S. Zhu, J. Zhang, C. Qiao, S. Tang, Y. Li, W. Yuan, B. Li, L. Tian, F. Liu, R. Hu, H. Gao, H. Wei, H. Zhang, H. Sun, B. Yang, Chem. Commun. 47 (2011) 6858–6860.
- [12] P. M. Carrasco, I. García, L. Yate, R. T. Zaera, G. Cabanero, H. J. Grande, V. Ruiz, Carbon 109 (2016) 658-665.
 [13] H. Chen, Z. Wang, S. Zong, P. Chen, D. Zhu, L. Wu, Y. Cui, Nanoscale 7 (2015) 15477-15486.
- [14] H. Li, X. He, Z. Kang, H. Huang, Y. Liu, J. Liu, S. Lian, C. H. A. Tsang, X. Yang, S. Lee, Angew. Chem. Int. Ed. 49 (2010) 4430-4434.
- [15] L. Peng, Z. Zhang, C. Qiu, Nat. Electron. 2 (2019) 499-505
- [16] L. Sun, X. Wang, Y. Wang, Q. Zhang, Carbon 122 (2017) 462-474.
- [17] S. Peretz, O. Regev, Curr. Opin. Colloid Interface Sci. 17 (2012) 360-368.
- [18] M. F. L. De Volder, S. H. Tawfick, R. H. Baughman, A. J. Hart, Science 339 (2013) 535-539.
- [19] Z. M. Markovic, B. Z. Ristic, K. M. Arsikin, D. G. Klisic, L. M. H. Trajkovic, B. M. T. Markovic, D. P. Kepic, T. K. K. Stevovic, S. P. Jovanovic, M. M. Milenkovic, D. D. Milivojevic, V. Z. Bumbasirevic, M. D. Dramicanin, V. S. Trajkovic, Biomaterials 33 (2012) 7084-7092.

- [20] X. Xu, R. Ray, Y. Gu, H. J. Ploehn, L. Gearheart, K. Raker, W. A. Scrivens, J. Am. Chem. Soc. 126 (2004) 12736-12737.
- [21] J. Moon, J. An, U. Sim, S. P. Cho, J. H. Kang, C. Chung, J. H. Seo, J. Lee, K. T. Nam, B. H. Hong, Adv. Mater. 26 (2014) 3501-3505.
- [22] A. Ciesielski, S. Haar, A. Aliprandi, M. E. Garah, G. Tregnago, G. F. Cotella, M. E. Gemayel, F. Richard, H. Sun, F. Cacialli, F. Bonaccorso, P. Samorì, ACS Nano 10 (2016) 10768-10777.
- [23] J. Zhou, C. Booker, R. Li, X. Zhou, T. K. Sham, X. Sun, Z. Ding, J. Am. Chem. Soc. 129 (2007) 744-745.
- [24] Z. Luo, G. Qi, K. Chen, M. Zou, L. Yuwen, X. Zhang, W. Huang, L. Wang, Adv. Funct. Mater. 26 (2016) 2739-2744.
 [25] Y. Yin, Q. Liu, D. Jiang, X. Du, J. Qian, H. Mao, K. Wang, Carbon 96 (2016) 1157-1165.
- [26] M. H. Tran, T. Park, J. Hur, Appl. Surf. Sci. 539 (2021) 148222.
- [27] A. B. Bourlinos, A. Stassinopoulos, D. Anglos, R. Zboril, V. Georgakilas, E. P. Giannelis, Chem. Mater. 20 (2008) 4539-4541.
- [28] J. M. Ha, N. E. Lee, Y. J. Yoon, S. H. Lee, Y. S. Hwang, J. K. Suk, C. Y. Lee, C. R. Kim, S. Yeo, Carbon 186 (2022) 28-35.